

## Two-band superfluidity from the BCS to the BEC limit

M. Iskin and C. A. R. Sá de Melo

*School of Physics, Georgia Institute of Technology, Atlanta, Georgia 30332, USA*

(Dated: August 26, 2018)

We analyze the evolution of two-band superfluidity from the weak coupling Bardeen-Cooper-Schrieffer (BCS) to the strong coupling Bose-Einstein condensation (BEC) limit. When the interband interaction is tuned from negative to positive values, a quantum phase transition occurs from a 0-phase to a  $\pi$ -phase state, depending on the relative phase of two order parameters. Furthermore, population imbalances between the two bands can be created by tuning the intraband or interband interactions. We also find two undamped low energy collective excitations corresponding to in-phase and out-of-phase modes. Lastly, we derive the coupled Ginzburg-Landau equations, and show that they reduce to coupled Gross-Pitaevskii equations for two types of bosons in the BEC limit.

PACS numbers: 03.75.Ss, 03.75.Hh, 05.30.Fk

A two-band theory of superconductivity was introduced by Suhl et al. [1] in 1959 soon after the Bardeen-Cooper-Schrieffer (BCS) theory to allow for the possibility of multiple band crossings at the Fermi surface. This model has been applied to high- $T_c$  superconductors and  $\text{MgB}_2$ , where, in the latter case, experimental properties can be well described by a two-band weak coupling BCS theory [2, 3, 4, 5]. Unfortunately, interband or intraband interactions can not be tuned in these condensed matter systems, and their properties can not be studied away from the BCS regime. However, two-band fermions may also be produced experimentally with ultracold atomic Fermi gases in optical lattices [6] or in single traps of several hyperfine states. In this case, (intraband and interband) interactions may be tuned using Feshbach resonances which allow for the study of the evolution of two-band superfluidity from the BCS to the Bose-Einstein condensation (BEC) limit. The BCS to BEC evolution in the two-band problem is much richer than the one-band case which has already been experimentally studied [6, 7, 8, 9, 10, 11, 12], since additional interaction parameters (interband and intraband) may be controlled externally.

Furthermore, a two-band model may be used not only to describe experiments involving several hyperfine states of the same fermion, but also may be used to study two different fermionic species (e.g.  $^6\text{Li}$  and  $^{40}\text{K}$ ). In systems involving mixtures of two different alkali atoms, simple one-band theories may not be sufficient to describe the interactions between the two species of atoms, and two-band theories may be necessary to model future experiments. Thus, due to recent developments and advances in atomic physics described above, and in anticipation of future experiments, we describe here the BCS to BEC evolution of two-band superfluids for all coupling strengths at zero and finite temperatures.

The main results of our paper are as follows. We show that a quantum phase transition occurs from a 0-phase to a  $\pi$ -phase state (depending on the relative phase of the order parameters of the two-bands) when the interband

interaction  $J$  is tuned from negative to positive values. We found that population imbalances between the two bands can be created by tuning intraband or interband interactions. In addition, we describe the evolution of two undamped low energy collective excitations corresponding to in-phase phonon (or Goldstone) and out-of-phase exciton (finite frequency) modes. Near the critical temperature, we derive the coupled Ginzburg-Landau (GL) equations for a two-band superfluid, and show that they reduce to coupled Gross-Pitaevskii (GP) equations for two types of composite bosons in strong coupling.

In order to obtain the results described above, we start from a generalized Hamiltonian for multi-band superfluids with spin (pseudo-spin) singlet pairing

$$H = \sum_{n,\mathbf{k},\sigma} \xi_{n,\sigma}(\mathbf{k}) a_{n,\sigma}^\dagger(\mathbf{k}) a_{n,\sigma}(\mathbf{k}) - \sum_{n,m,r,s,\mathbf{q}} V_{nm}^{rs} b_{nm}^\dagger(\mathbf{q}) b_{rs}(\mathbf{q}), \quad (1)$$

where the indices  $n, m, r$  and  $s$  label different energy bands (or components), and  $\sigma$  labels spins (or pseudo-spins). The operators  $a_{n,\uparrow}^\dagger(\mathbf{k})$  and  $b_{nm}^\dagger(\mathbf{q}) = \sum_{\mathbf{k}} \Gamma_{nm}^*(\mathbf{k}) a_{n,\uparrow}^\dagger(\mathbf{k} + \mathbf{q}/2) a_{m,\downarrow}^\dagger(-\mathbf{k} + \mathbf{q}/2)$  create a single and a pair of fermions, respectively. The symmetry factor  $\Gamma_{nm}(\mathbf{k})$  characterizes the chosen angular momentum channel, where  $\Gamma_{nm}(\mathbf{k}) = k_{nm,0}/(k_{nm,0}^2 + k^2)^{1/2}$  is for the  $s$ -wave interaction in three dimensions. Here,  $k_{nm,0} \sim R_{nm,0}^{-1}$  sets the scale at small and large momenta, where  $R_{nm,0}$  plays the role of the interaction range. In addition  $\xi_{n,\sigma}(\mathbf{k}) = \epsilon_n(\mathbf{k}) - \mu_{n,\sigma}$ , where  $\epsilon_n(\mathbf{k}) = \epsilon_{n,0} + k^2/(2M_n)$  is the kinetic energy ( $\hbar = 1$ ) and  $M_n$  is the band mass of the fermions.

From now on, we focus on a two-band system such that  $V_{nm}^{rs} = V_{nr} \delta_{nm} \delta_{rs}$  with distinct intraband ( $V_{11}, V_{22}$ )  $> 0$  and interband ( $V_{12} = V_{21} = J$ ) interactions. Notice that,  $J$  plays the role of the Josephson interaction which couples the two energy bands. In addition, we assume that the total number of fermions is fixed ( $N = N_1 + N_2$ ) such that the chemical potentials of fermions are

identical ( $\mu_{n,\sigma} = \mu$ ), and that the reference energies are such that  $\epsilon_{1,0} = 0$  and  $\epsilon_{2,0} = \epsilon_D > 0$ , as shown in Fig. 1a. Here,  $\epsilon_D = k_D^2/(2M_1) \leq \epsilon_F = k_{1,F}^2/(2M_1)$ , where  $\epsilon_F$  is the Fermi energy and  $k_{n,F}$  are the Fermi momenta  $k_{1,F} = k_F$  and  $k_{2,F} = [2M_2(\epsilon_F - \epsilon_D)]^{1/2}$ . Since the low energy physics depends weakly on  $k_{n,0}$  in dilute systems ( $\mathcal{N}R_0^3 \ll 1$ ) characterized by  $k_{n,0}^3 \gg k_{n,F}^3$  where  $\mathcal{N} = N/\mathcal{V}$  is the density of fermions and  $\mathcal{V}$  is the volume, we assume for simplicity that  $k_{n,0} = k_0 \gg k_F$ .

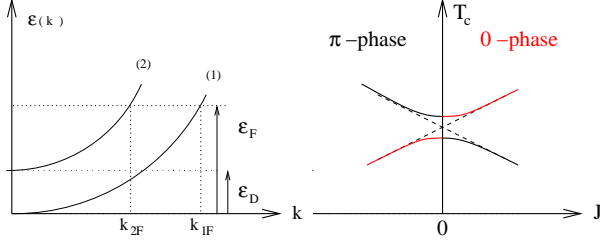


FIG. 1: Schematic (a) figure of two bands with reference energies  $\epsilon_{1,0} = 0$  and  $\epsilon_{2,0} = \epsilon_D$ , and (b) phase diagram of 0-phase and  $\pi$ -phase states.

The gaussian action for  $H$  is ( $k_B = 1, \beta = 1/T$ )

$$S_{\text{gauss}} = S_0 + \frac{\beta}{2} \sum_q \Lambda^\dagger(-q) \mathbf{F}^{-1}(q) \Lambda(q), \quad (2)$$

where  $q = (\mathbf{q}, i\nu_\ell)$  denotes both momentum and bosonic Matsubara frequency  $\nu_\ell = 2\ell\pi/\beta$ . Here, the vector  $\Lambda^\dagger(-q) = [\Lambda_1^\dagger(q), \Lambda_1(-q), \Lambda_2(-q), \Lambda_2^\dagger(q)]$  is the order parameter fluctuation field, and the matrix  $\mathbf{F}^{-1}(q)$  is the inverse fluctuation propagator. The saddle point action is  $S_0 = -\beta \sum_{n,m} g_{nm} \Delta_{n,0}^* \Delta_{m,0} + \sum_{n,\mathbf{k}} \{\beta[\xi_n(\mathbf{k}) - E_n(\mathbf{k})] - 2 \ln[1 + \exp(-\beta E_n(\mathbf{k}))]\}$ , where  $g_{11} = -V_{22}/\det \mathbf{V}$ ,  $g_{22} = -V_{11}/\det \mathbf{V}$  and  $g_{12} = g_{21} = J/\det \mathbf{V}$  with  $\det \mathbf{V} = V_{11}V_{22} - J^2 > 0$ . Here,  $E_n(\mathbf{k}) = [\xi_n^2(\mathbf{k}) + |\Delta_n(\mathbf{k})|^2]^{1/2}$  is the energy of the quasiparticles and  $\Delta_n(\mathbf{k}) = \Delta_{n,0} \Gamma_n(\mathbf{k})$  is the order parameter.

The action given in Eq. (2) leads to the thermodynamic potential  $\Omega_{\text{gauss}} = \Omega_0 + \Omega_{\text{fluct}}$ , where  $\Omega_0 = S_0/\beta$  is the saddle point and  $\Omega_{\text{fluct}} = \beta^{-1} \sum_q \ln \det[\mathbf{F}^{-1}(q)/(2\beta)]$  is the fluctuation contribution to  $\Omega_{\text{gauss}}$ . Expressing  $\Delta_{n,0}$  in terms of its amplitude and phase  $\Delta_{n,0} = |\Delta_{n,0}| \exp(i\varphi_n)$  shows explicitly the Josephson coupling energy  $[V_{22}|\Delta_{1,0}|^2 + V_{11}|\Delta_{2,0}|^2 - 2J|\Delta_{1,0}\Delta_{2,0}| \cos(\varphi_2 - \varphi_1)]/\det \mathbf{V}$  of  $\Omega_0$ . When  $J > 0$ , only the 0-phase (or in phase)  $\varphi_2 = \varphi_1$  solution is stable. However, when  $J < 0$ , only the  $\pi$ -phase (or out of phase)  $\varphi_2 = \varphi_1 + \pi$  solution is stable. Thus, a phase transition occurs from the 0-phase to the  $\pi$ -phase when the sign of  $J$  is tuned from negative to positive values as shown in Fig. 1b.

From the stationary condition  $\partial S_0/\partial \Delta_n^*(q) = 0$ , we obtain the order parameter equation

$$\begin{pmatrix} O_{11} & O_{12} \\ O_{21} & O_{22} \end{pmatrix} \begin{pmatrix} \Delta_{1,0} \\ \Delta_{2,0} \end{pmatrix} = 0, \quad (3)$$

where the matrix elements are given by  $O_{nm} = -g_{nm} - \delta_{nm} \sum_{\mathbf{k}} |\Gamma_n(\mathbf{k})|^2 \tanh[\beta E_n(\mathbf{k})/2]/[2E_n(\mathbf{k})]$ . Here,  $\delta_{nm}$  is the Kronecker delta. Notice that the order parameter amplitudes are the same for both the 0-phase and  $\pi$ -phase as can be shown directly from Eq. (3), but their relative phases are either 0 or  $\pi$ . In what follows, we analyse only the 0-phase state, keeping in mind that analogous results (with appropriate relative phase changes) apply to the  $\pi$ -phase state. We can eliminate  $V_{nn}$  in favor of scattering length  $a_{nn}$  via the relation  $1/V_{nn} = -M_n \mathcal{V}/(4\pi a_{nn}) + \sum_{\mathbf{k}} |\Gamma_n(\mathbf{k})|^2/[2\epsilon_n(\mathbf{k})]$ , which can be solved to obtain  $1/(k_{n,F} a_{nn}) = k_0/k_{n,F} - 4\pi/(k_{n,F} V_{nn} M_n \mathcal{V})$ .

The order parameter equation needs to be solved self-consistently with the number equation  $N = -\partial \Omega/\partial \mu$  leading to  $N_{\text{gauss}} = N_0 + N_{\text{fluct}}$ , and is given by

$$N_{\text{gauss}} = \sum_{\mathbf{k}, \sigma, m} \mathcal{N}_{0,m}(\mathbf{k}) - \frac{1}{\beta} \sum_q \frac{\partial[\det \mathbf{F}^{-1}(q)]/\partial \mu}{\det \mathbf{F}^{-1}(q)}. \quad (4)$$

Here, the first term is the saddle point ( $N_1 + N_2$ ) and the second term is the fluctuation ( $N_{\text{fluct}}$ ) contribution, where  $\mathcal{N}_{0,m} = 1/2 - \xi_m(\mathbf{k}) \tanh[\beta E_m(\mathbf{k})/2]/[2E_m(\mathbf{k})]$  is the momentum distribution. The inclusion of  $N_{\text{fluct}}$  is very important near the critical temperature, however,  $N_0$  may be sufficient at low temperatures [13, 14]. Next, we discuss the  $T = 0$  case.

In weak coupling ( $\max\{|\Delta_{1,0}|, |\Delta_{2,0}|\} \ll \epsilon_F$ ), the solutions of the order parameter equation are  $\max\{|\Delta_{1,0}|, |\Delta_{2,0}|\} \sim 8\epsilon_F \exp[-2 + \pi k_0/(2k_F) - \phi_-]$  and  $\min\{|\Delta_{1,0}|, |\Delta_{2,0}|\} \sim 8\epsilon_F \exp[-2 + \pi k_0/(2k_F) - \phi_+]$ , while the number equation leads to  $\mu \approx \epsilon_F$ . Here  $\phi_{\pm} = \lambda_{\pm} \pm [\lambda_{\pm}^2 - 1/\det \lambda]^{1/2}$  where  $\lambda_{\pm} = (\lambda_{11} \pm \lambda_{22})/(2 \det \lambda)$ ,  $\det \lambda = \lambda_{11}\lambda_{22} - \lambda_{12}\lambda_{21}$ , and  $\lambda_{nm} = V_{nm} D_m$  are the dimensionless interaction parameters with  $D_m = M_m \mathcal{V} k_{m,F}/(2\pi^2)$  is the density of states per spin at the Fermi energy. On the other hand, in strong coupling ( $\mu < 0$  and  $\max\{|\Delta_{1,0}|, |\Delta_{2,0}|\} \ll |\mu| \ll \epsilon_0$ ), the solution of the order parameter equations is  $\mu = -\epsilon_0 [\pi k_0/(2k_F \phi_+) - 1]^2$ , while the number equation leads to  $|\Delta_{m,0}|^2 = (8\pi \mathcal{N}_m/M_m) \sqrt{|\mu|/(2M_m)}$ . Here,  $\epsilon_0 = k_0^2/(2M_1)$  and  $\mathcal{N}_m = N_m/\mathcal{V}$ . Notice that the total density of fermions is  $\mathcal{N} = \mathcal{N}_1 + \mathcal{N}_2 = (k_{1,F}^3 + k_{2,F}^3)/(3\pi^2)$ . The familiar one-band results are recovered when  $J \rightarrow 0$  upon the use of the relation between  $V_{nn}$  and  $a_{nn}$ . Next, we analyze the  $T = 0$  evolution from BCS to BEC for identical bands ( $M_1 = M_2 = M$ ) with zero offset ( $\epsilon_D = 0$ ). For this purpose, we set  $k_0 \approx 256k_F$  and  $V_{22} = 0.001$  in units of  $5.78/(Mk_F \mathcal{V})$  [or  $1/(k_F a_{22}) \approx -3.38$ ], and analyze two cases.

In the first case, we solve for  $\mu$ ,  $|\Delta_{1,0}|$  and  $|\Delta_{2,0}|$  as a function of  $V_{11}$  [or  $1/(k_F a_{11})$ ], and show  $\Delta_{n,0}$  in Fig. 2a for fixed values of  $J$ . The unitarity limit is reached at  $V_{11} \approx 1.0132V_{22}$  [or  $1/(k_F a_{11}) \approx 0$ ] while  $\mu$  changes sign at  $V_{11} \approx 1.0159$  [or  $1/(k_F a_{11}) \approx 0.69$ ]. The evolution of  $|\Delta_{1,0}|$  is similar to the one band result [13] where it

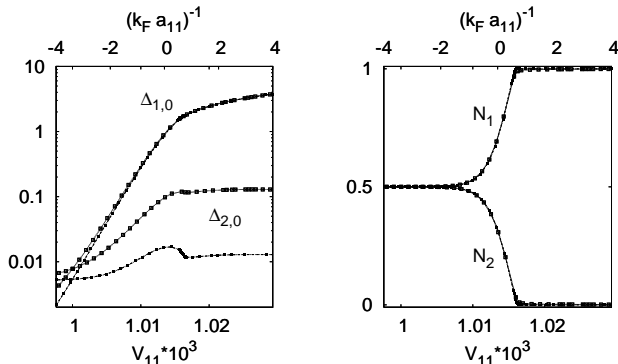


FIG. 2: Plots of (a) order parameter amplitude  $|\Delta_{n,0}|$  (in units of  $\epsilon_F$ ), and (b) fraction of fermions  $N_n/N$  versus  $V_{11}$  [in units of  $5.78/(Mk_F\mathcal{V})$ ] and versus  $1/(k_F a_{11})$  for  $J = 0.001V_{22}$  (hollow squares) and  $J = 0.0001V_{22}$  (solid squares).

grows monotonically with increasing  $V_{11}$ . However, the evolution of  $|\Delta_{2,0}|$  is non-monotonic where it has a hump approximately  $V_{11} \approx 1.0155V_{22}$  [or  $1/(k_F a_{11}) \approx 0.58$ ], and it decreases for stronger interactions until it vanishes (not shown). In Fig. 2b, we show that both bands have similar populations for  $V_{11} \sim V_{22}$ . However, as  $V_{11}/V_{22}$  increases, fermions from the second band are transferred to the first, where bound states are easily formed and reduce the free energy.

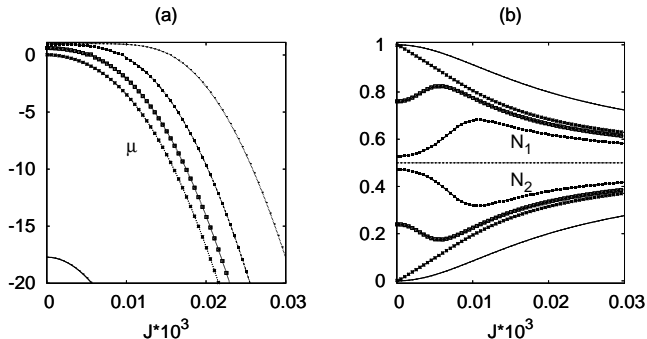


FIG. 3: Plots of (a) chemical potential  $\mu$  (in units of  $\epsilon_F$ ), and (b) fraction of fermions  $N_n/N$  versus  $J$  [in units of  $5.78/(Mk_F\mathcal{V})$ ] for  $V_{11} = \gamma V_{22}$  where  $\gamma = 1$  (dotted lines), 1.010 (solid squares), 1.014 (hollow squares), 1.016 (crossed lines) and 1.030 (solid lines); or  $1/(k_F a_{11}) \approx -3.38, -0.81, 0.20, 0.70$  and  $4.17$ , respectively.

In the second case, we solve for  $\mu$ ,  $|\Delta_{1,0}|$  and  $|\Delta_{2,0}|$  as a function of  $J$ , and show  $\mu$  in Fig. 3a for fixed values of  $V_{11}/V_{22}$ . The order parameters  $|\Delta_{1,0}|$  and  $|\Delta_{2,0}|$  grow with increasing  $J$  (not shown). In Fig. 3b, we show that the band populations  $N_1$  and  $N_2$  for several values of  $\gamma$ . Notice the population imbalance and the presence of maxima (minima) in  $N_1$  ( $N_2$ ) for finite  $J$ , which is associated with the sign change of  $\mu$  shown in Fig. 3a. When  $V_{11} > V_{22}$ , there is population imbalance even for  $J = 0$ , because atom pairs can be easily transferred from

the second band to the first until an optimal  $J_o$  is reached. Further increase in  $J$  produces also transfer from the first band to the second leading to similar populations for  $J \gg J_o$ .

Next, we discuss the low energy collective excitations at  $T = 0$ , which are determined by  $\det \mathbf{F}^{-1}(q) = 0$ . The phase-only collective excitations in weak and strong couplings lead to a Goldstone mode  $w^2(\mathbf{q}) = v^2|\mathbf{q}|^2$  characterized by the speed of sound  $v^2 = (D_1v_1^2 + D_2v_2^2)/(D_1 + D_2)$ ; and a finite frequency mode  $w^2(\mathbf{q}) = w_0^2 + u^2|\mathbf{q}|^2$  characterized by the finite frequency  $w_0^2 = 4\alpha|g_{12}\Delta_{1,0}\Delta_{2,0}|\sqrt{\epsilon_F/|\mu|}(D_1 + D_2)/(D_1D_2)$  and the speed  $u^2 = (D_1v_2^2 + D_2v_1^2)/(D_1 + D_2)$ . In weak coupling,  $\alpha = 1$  and  $v_n = v_{n,F}/\sqrt{3}$ , while  $\alpha = 1/\pi$  and  $v_n = |\Delta_{n,0}|/\sqrt{8M_n|\mu|}$  in strong coupling. Here,  $v_{n,F}$  is the Fermi velocity. It is also illustrative to analyse the eigenvectors associated with these solutions in weak and strong couplings. In the limit of  $\mathbf{q} \rightarrow 0$ , we obtain  $(\theta_1, \theta_2) \propto (|\Delta_{1,0}|, |\Delta_{2,0}|)$  for the Goldstone mode corresponding to an in-phase solution, while  $(\theta_1, \theta_2) \propto (D_2|\Delta_{1,0}|, -D_1|\Delta_{2,0}|)$ , for the finite frequency mode corresponding to an out-of-phase solution. Our findings generalize Leggett's weak coupling results [15, 16].

Next, we discuss two band superfluidity near the critical temperature  $T_c$ , where  $|\Delta_{1,0}| \sim |\Delta_{2,0}| \rightarrow 0$ . For  $T = T_c$ , the order parameter equation reduces to

$$\det \mathbf{O} = O_{11}O_{22} - O_{12}O_{21} = 0, \quad (5)$$

and the saddle point number equation  $N_0 = \sum_{\mathbf{k}, n} n_F[\xi_n(\mathbf{k})]$  corresponds to the number of unbound fermions, where  $n_F(x) = 1/[\exp(\beta x) + 1]$  is the Fermi distribution. While  $N_0$  is sufficient in weak coupling, the inclusion of  $N_{\text{fluct}}$  is crucial in strong couplings, and can be obtained as follows. Near  $T = T_c$ , the fluctuation action  $S_{\text{fluct}}$  reduces to  $S_{\text{fluct}} = (\beta/2) \sum_{q, n, m} L_{nm}^{-1}(q) \Lambda_n^*(q) \Lambda_m(q)$  where

$$L_{nn}^{-1} = -g_{nn} - \sum_{\mathbf{k}} \frac{1 - n_F(\xi_{n+}) - n_F(\xi_{n-})}{\xi_{n+} + \xi_{n-} - iv_\ell} |\Gamma_n(\mathbf{k})|^2 \quad (6)$$

corresponds to the fluctuation propagator of band  $n$ ,  $L_{n \neq m}^{-1}(q) = g_{nm}$ , and  $\xi_{n\pm} = \xi_n(\mathbf{k} \pm \mathbf{q}/2)$ . Thus, the resulting action leads to  $\Omega_{\text{fluct}} = \beta^{-1} \sum_q \ln[\det \mathbf{L}^{-1}(q)/\beta^2]$ , where  $\det \mathbf{L}^{-1}(q) = L_{11}^{-1}(q)L_{22}^{-1}(q) - g_{12}g_{21}$ . Notice that,  $\det \mathbf{L}^{-1}(0) = 0$  also produces Eq. (5), which is the Thouless condition. After the analytic continuation  $iv_\ell \rightarrow w + i0^+$ , we expand  $L_{nn}^{-1}(q)$  to first order in  $w$  and second order in  $\mathbf{q}$  such that  $L_{nn}^{-1}(q) = a_n + \sum_{i,j} c_n^{ij} q_i q_j / (2M_n) - d_n w$ . The time-independent coefficients are given by  $a_n = -g_{nn} - \sum_{\mathbf{k}} X_n |\Gamma_n(\mathbf{k})|^2 / [2\xi_n(\mathbf{k})]$  and  $c_n^{ij} = \sum_{\mathbf{k}} \{X_n \delta_{ij} / [8\xi_n^2(\mathbf{k})] - \beta Y_n \delta_{ij} / [16\xi_n(\mathbf{k})] + \beta^2 X_n Y_n k_i k_j / [16M_n \xi_n(\mathbf{k})]\} |\Gamma_n(\mathbf{k})|^2$ , where  $X_n = \tanh[\beta \xi_n(\mathbf{k})/2]$  and  $Y_n = \text{sech}^2[\beta \xi_n(\mathbf{k})/2]$ . Notice that,  $c_n^{ij} = c_n \delta_{ij}$  is isotropic for the  $s$ -wave

considered here. The time-dependent coefficient has real and imaginary parts, and for the  $s$ -wave case is given by  $d_n = \sum_{\mathbf{k}} X_n |\Gamma_n(\mathbf{k})|^2 / [4\xi_n^2(\mathbf{k}) + i(\beta\pi/8)\epsilon_0 D_n \sqrt{\mu/\epsilon_F} \Theta(\mu)/(\epsilon_0 + \mu)]$ , where  $\Theta(x)$  is the Heaviside function. For completeness, we present the asymptotic forms of  $a_n, c_n$  and  $d_n$ . In weak coupling ( $\mu \approx \epsilon_F$ ), we find  $a_n = -g_{nn} + D_n [\ln(T/T_c) + \phi_-]$ ,  $c_n = 7\epsilon_F D_n \zeta(3)/(12T_c^2 \pi^2)$ , and  $d_n = D_n [1/(4\epsilon_F) + i/(8T_c)]$ , where  $\zeta(x)$  is the Zeta function, and  $T_c$  is the physical critical temperature. In strong coupling ( $\epsilon_0 \gg |\mu| \gg T_c$ ), we find  $a_n = -g_{nn} - \pi D_n \epsilon_0 / [2\sqrt{\epsilon_F} (\sqrt{|\mu|} + \sqrt{\epsilon_0})]$ ,  $c_n = \pi D_n / (16\sqrt{|\mu|\epsilon_F})$  and  $d_n = \pi D_n / (8\sqrt{|\mu|\epsilon_F})$ .

In order to obtain  $\Omega_{\text{fluct}}$ , there are two contributions, one from the scattering states and the other from poles of  $\mathbf{L}(q)$ . The pole contribution dominates in strong coupling. In this case, we evaluate  $\det \mathbf{L}^{-1}(q) = 0$  and find the poles  $w_{\pm}(\mathbf{q}) = A_{\pm} + B_{\pm} |\mathbf{q}|^2 \pm [(A_{-} + B_{-} |\mathbf{q}|^2)^2 + g_{12} g_{21} / (d_1 d_2)]^{1/2}$ , where  $A_{\pm} = (a_1 d_2 \pm a_2 d_1) / (2d_1 d_2)$  and  $B_{\pm} = (M_2 d_2 c_1 \pm M_1 d_1 c_2) / (4M_1 M_2 d_1 d_2)$ . Notice that, when  $J \rightarrow 0$ , we recover the limit of uncoupled bands with  $w_n(\mathbf{q}) = a_n/d_n + |\mathbf{q}|^2 c_n / (2M_n d_n)$ . In the  $\mathbf{q} \rightarrow 0$  limit, when  $J > 0$  ( $J < 0$ ), the eigenvectors  $[\Lambda_1^{\dagger}(0), \Lambda_2^{\dagger}(0)] = [g_{12}, a_1 - d_1 w_{\pm}(0)]$  correspond to an in-phase (out-of-phase) mode for  $w_{+}(\mathbf{q})$  and an out-of-phase (in-phase) mode for  $w_{-}(\mathbf{q})$ . Thus, we obtain  $\Omega_{\text{fluct}} = (1/\beta) \sum_{\pm, q} \ln[\beta(iv_{\ell} - w(\mathbf{q}))]$  which leads to

$$N_{\text{fluct}} = \sum_{\pm, \mathbf{q}} \frac{\partial w(\mathbf{q})}{\partial \mu} n_B[w(\mathbf{q})]. \quad (7)$$

For sufficiently strong couplings,  $\partial w_{\pm}(\mathbf{q})/\partial \mu = 2$ , and the poles can also be written as  $w_{\pm}(\mathbf{q}) = -\mu_{B, \pm} + |\mathbf{q}|^2 / (2M_{B, \pm})$ , where  $\mu_{B, \pm}$  is the chemical potential and  $M_{B, \pm}$  is the mass of the corresponding bosons. In the case of identical bands with zero offset,  $c_1 = c_2 = c$  and  $d_1 = d_2 = d$ ,  $\mu_{B, \pm} = -[a_1 + a_2 \pm \sqrt{(a_1 - a_2)^2 + 4g_{12}g_{21}}] / (2d)$  and  $M_{B, \pm} = 2M$  in strong coupling. Notice that the  $+$  bosons always condense first for any  $J$  (independent of its sign) since  $\mu_{B, +} \rightarrow 0$  first. Next, we analyze  $T_c$  in weak and strong couplings.

In weak coupling, solutions to the order parameter equation Eq. (5) are  $T_{c, \mp} = (8\epsilon_F/\pi) \exp[\gamma - 2 + \pi k_0 / (2k_F) - \phi_{\pm}]$ , while the number equation Eq. (4) leads to  $\mu \approx \epsilon_F$ . On the other hand, in strong coupling, the solution of the order parameter equation is  $\mu = -\epsilon_0 [\pi k_0 / (2k_F \phi_{+}) - 1]^2$ , while the number equation  $\mathcal{N}/2 = \mathcal{N}_{B, +} + \mathcal{N}_{B, -}$  with  $\mathcal{N}_{B, +} \gg \mathcal{N}_{B, -}$  leads to  $T_{c, +} = \pi \{ \mathcal{N}_{B, +} / [\zeta(3/2)(M_{B, +} \sqrt{M_{B, +}})] \}^{2/3}$ , since the  $+$  bosons condense first. Notice that, the physical critical temperature is  $T_c = \max\{T_{c, +}, T_{c, -}\} = T_{c, +}$  for any  $J$ . Therefore,  $T_c$  grows continuously from an exponential dependence on interaction to a constant BEC temperature.

Next, we obtain the TDGL equations for  $T \approx T_c$ ,

$$\left[ a_n + b_n |\Lambda_n(x)|^2 - \frac{c_n}{2M_n} \nabla^2 - id_n \frac{\partial}{\partial t} \right] \Lambda_n(x)$$

$$+ g_{n \neq m} \Lambda_m(x) = 0, \quad (8)$$

in the real space  $x = (\mathbf{x}, t)$  representation. The coefficient of the nonlinear term  $b_n = \sum_{\mathbf{k}} \{ X_n / [4\xi_n^3(\mathbf{k}) - \beta Y_n / [8\xi_n^2(\mathbf{k})]] \} |\Gamma_n(\mathbf{k})|^4$  can also be obtained analytically in weak  $b_n = 7D_n \zeta(3) / (8T_c^2 \pi^2)$  and strong  $b_n = \pi D_n / (4|\mu| \sqrt{2|\mu|\epsilon_F})$  coupling limits. In weak coupling, Eq. (8) reduces to the coupled GL equations of two BCS type superconductors. However, in strong coupling, it is more illustrative to derive TDGL equations in the rotated basis of  $+$  and  $-$  bosons  $(\Phi_{+}^{\dagger}, \Phi_{-}^{\dagger}) = (\Lambda_1^{\dagger}, \Lambda_2^{\dagger}) \mathbf{R}^{\dagger}$ , where  $\mathbf{R}$  is the unitary matrix that diagonalizes the linear part of the TDGL equations. In this basis, Eq. (8) reduces to generalized GP equations of  $\Phi_{+}$  and  $\Phi_{-}$  bosons showing explicitly terms coming from density-density interactions such as  $U_{\pm\pm} |\Phi_{\pm}|^2 \Phi_{\pm}$  or  $U_{\pm\mp} |\Phi_{\pm}|^2 \Phi_{\mp}$ . In the case of identical bands with zero offset, this leads to  $U_{++} = U_{--} = b/(2d^2)$  and  $U_{+-} = U_{-+} = 3b/(2d^2)$  as the repulsive density-density interactions.

In conclusion, we showed that a quantum phase transition occurs from a 0-phase to a  $\pi$ -phase state depending on the relative phase of the two order parameters, when the interband interaction  $J$  is tuned from negative to positive values. We found that population imbalances between the two bands can be created by tuning intra-band or interband interactions. In addition, we described the evolution of two undamped low energy collective excitations corresponding to in-phase phonon (or Goldstone) and out-of-phase exciton (finite frequency) modes. Near the critical temperature, we derived the coupled Ginzburg-Landau (GL) equations for a two-band superfluid, and showed that they reduce to coupled Gross-Pitaevskii (GP) equations for two types of composite bosons in strong coupling.

We thank NSF (DMR-0304380) for support.

- 
- [1] H. Suhl et al., Phys. Rev. Lett. **3**, 552 (1959).
  - [2] M. Iavarone et al., Phys. Rev. Lett. **89**, 187002 (2001).
  - [3] F. Bouquet et al., Phys. Rev. Lett. **89**, 257001 (2002).
  - [4] S. Tsuda et al., Phys. Rev. Lett. **91**, 127001 (2003).
  - [5] J. Geerk et al., Phys. Rev. Lett. **94**, 227005 (2005).
  - [6] M. Köhl et al., Phys. Rev. Lett. **94**, 080403 (2005).
  - [7] K. E. Strecker et al., Phys. Rev. Lett. **91**, 080406 (2003).
  - [8] C. A. Regal et al., Phys. Rev. Lett. **92**, 040403 (2004).
  - [9] M. Bartenstein et al., Phys. Rev. Lett. **92**, 120401 (2004).
  - [10] J. Kinast et al., Phys. Rev. Lett. **92**, 150402 (2004).
  - [11] T. Bourdel et al., Phys. Rev. Lett. **93**, 050401 (2004).
  - [12] M. W. Zwierlein et al., Nature **435**, 1047 (2005).
  - [13] C. A. R. Sá de Melo et al., Phys. Rev. Lett. **71**, 3202 (1993).
  - [14] J. R. Engelbrecht et al., Phys. Rev. B **55**, 15153 (1997).
  - [15] A. J. Leggett, Progr. Theor. Phys. **36**, 901 (1966).
  - [16] M. Iskin and C. A. R. Sá de Melo, Phys. Rev. B **72**, 024512 (2005).